Sensors & Actuators: B. Chemical 295 (2019) 30–39

Contents lists available at ScienceDirect

Sensors and Actuators B: Chemical

journal homepage: www.elsevier.com/locate/snb

Chip modularity enables molecular information access from organ-on-chip devices with quality control

Wu Shang[a], Chen-Yu Chen[a,b,c], Kimberly Lo[a], Gregory F. Payne[a,b,c], William E. Bentley[a,b,c,*]

[a] Fischell Department of Bioengineering, University of Maryland, College Park, MD, 20742, United States
[b] Institute for Bioscience and Biotechnology Research, University of Maryland, College Park, MD, 20742, United States
[c] Robert E. Fischell Institute for Biomedical Devices, University of Maryland, College Park, MD, 20742, United States

ARTICLE INFO

Keywords:
Biofabrication
Electrochemical assays
Redox
Cytotoxicity
Microfluidics
Modularity

ABSTRACT

Organ-on-chip (OOC) devices are envisioned to replace animal models in preclinical toxicity and efficacy testing. Although significant progress has been made towards ensuring the biofidelity of these devices, analyzing samples from within these miniaturized structures remains a challenge. Based on the concept of modularity, we developed accessorial modular functional units that facilitate molecular information access to and from OOCs. Specifically, we developed three mutually independent microfluidic modules: a mixer, a "molecular-electronic" sensor, and a quality control unit. Each module can be interconnected/disconnected, replicated or replaced as needed. As a proof of concept, we developed a cytotoxicity assay comprised of two modules and linked these to a model OOC providing near real time molecular information on OOC function. Additionally, we developed sensor design criteria for generic use, particularly for on-chip measurements that require substrates and enzymes. We monitored sensor function during long-term experiments and, by design, maintained assay consistency by switching out fouled sensors. Importantly, using electrobiofabrication, our sensor assembly with biological components and its connection to the OOC requires only minutes and no bulky instrumentation. We believe a modular strategy wherein various chips are assembled *in situ* and subsequently interrogated in real time could provide an alternative and promising path to enhance functionality, reproducibility, and utility. They will enrich our abilities to access biological information in a variety of contexts.

1. Introduction

Organ-on-chips (OOCs) are gaining acceptance as *in vitro* models that would ultimately replace animal testing during drug development ([1–3,4–7]). In addition to the obvious ethical benefits, these miniaturized devices offer numerous advantages over traditional animal models including, reduced sample quantity and the ability to integrate various cell and tissue types in dynamic 3D microenvironments. Significant effort has been devoted to recapitulate human tissue-/organ-level physiologies to improve the fidelity of OOCs which, in turn, helps to minimize translational barriers for their use. Yet, information access from such miniaturized structures remains a challenge. Optical measurements are incorporated that often produce end-point data; their labeling processes can also be detrimental to cell cultures [2,3,7–9]. Recently, analytical interrogation using microelectronics-based sensors has opened an alternative modality for data acquisition. With benefits of high detection sensitivity and high versatility, these sensors have been patterned into OOCs for analyzing tissue barrier integrity [10], cell migration [11], fluid pressure [12] and oxygen [13]. We note, however, the embedded integration of sensors can significantly increase the complexity of OOC design and fabrication and this can hamper the translation of these technologies from lab to industry [14–21]. In addition, chemicals involved with many sensors can exhibit toxicity to cell cultures [2,3,22,23]. Moreover, issues involving sensor shelf life and quality control further complicate assay consistency during long-term testing [24,25].

Here, we apply the concept of device modularity to facilitate information access from OOCs while circumventing many of the aforementioned concerns. Instead of monolithic OOCs with integrated sensors, we develop three categories of accessorial modular units, each with a unique functionality: input (*e.g.*, medium/drug introduction), output (*i.e.*, sample analysis), and quality control (QC) (Scheme 1A). All modules are mutually independent and can be interconnected/disconnected, replicated or replaced in an analogous manner to Lego™, but

* Corresponding author at: Fischell Department of Bioengineering, University of Maryland, College Park, MD, 20742, United States.
E-mail addresses: shangwu563438@gmail.com (W. Shang), cchen634@umd.edu (C.-Y. Chen), klo1@umd.edu (K. Lo), gpayne@umd.edu (G.F. Payne), bentley@umd.edu (W.E. Bentley).

https://doi.org/10.1016/j.snb.2019.05.030
Received 19 January 2019; Received in revised form 5 April 2019; Accepted 9 May 2019
Available online 15 May 2019
0925-4005/

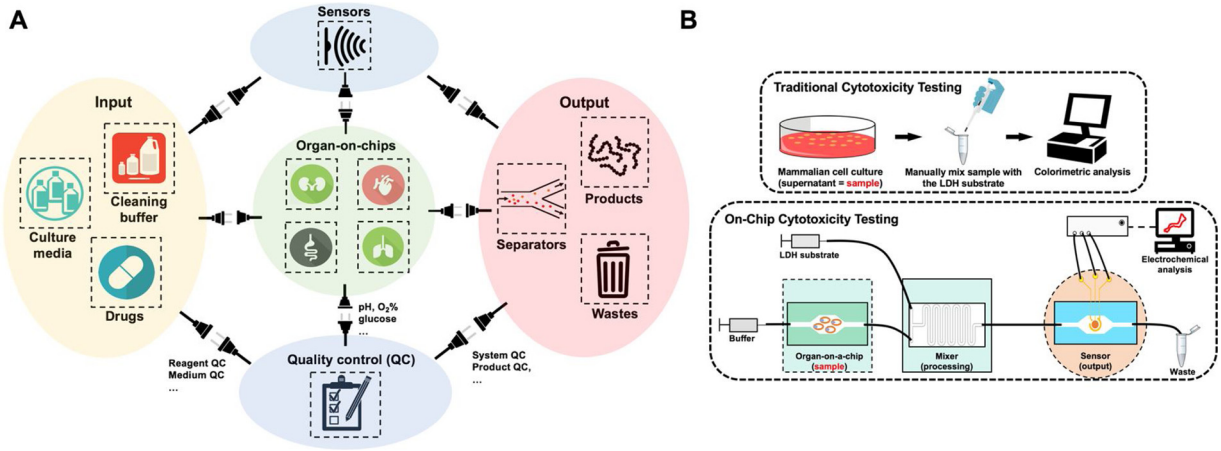

Scheme 1. Schematic of modular connected organ-on-chips (OOC) system. (A) Modules can be reversibly assembled in an analogous manner to Lego™, but connected using microtubing. "Input" modules can be placed upstream to OOCs to supply culture media for cell cultivation, introduce drug for screening, or even flush the system with cleaning buffer. Effluent from OOCs can be exported into "output" modules, wherein analytes of interest can be separated and sorted. In the case of a bioreactor, cellular products can also be collected using output modules. Sensors can be designed to collect information from all modules. Most importantly, the flexibility of modular assembly enables the design of unique modular functions to conduct quality control (QC) tests on each component in the system. That is, QC modules can be applied to monitor the function of system components ranging from input modules (*e.g.*, medium quality, reagent activity), OOCs (*e.g.*, pH, glucose, dissolved O2 level), output modules (*e.g.*, separator function, product quality), and to the function of sensors (not shown in schematic). (B) Schematic illustrating differences in cytotoxicity assays for use in traditional cell culture using commercialized LDH kits and for OOCs using programmable modular microfluidic systems.

connected using microtubing. Upon connection, the accessorial modules process information from the target OOC without increasing its complexity. To demonstrate this concept, the modular units are devised to evaluate culture cytotoxicity, which is traditionally measured manually, involves sample preparation, and utilizes relatively large sample volumes (Scheme 1B). Here, a fluid sample from a model OOC (cell culture in a simple 2D microdevice that contains a to-be-assayed enzyme) is first transferred in parallel with enzyme substrate into a mixer module where it is converted to a final product that is then detected by a sensor module downstream. The entire process, with the exception of attaching modules with tubing, is entirely hands-free. Specifically, a redox-based sensor was developed to measure the activity of a cell death biomarker, lactate dehydrogenase (LDH). We show how this cytotoxicity assay works using a model cell line, human colorectal adenocarcinoma cells (Caco-2 cell), disturbed by a drug mimic (*e.g.*, Triton X-100). By design, modular microfluidics help to exclude the introduction of detrimental chemicals to sensor modules (*e.g.*, lactate ([26–29]) and keep sensor-specific species such as catechol ([30,31])) from interfering with the cell cultures. Another strength for including modularity is that each module may be individually replaced or switched on the basis of the need, which makes the design more flexible and cost-efficient [32] as well as it facilitates long-term maintenance and monitoring [33,34]. By switching the OOC to a QC module, sensor function (often exhibiting declining sensitivity due to fouling [35]) can be repeatedly monitored during long-term experiments. Perhaps more importantly, assay consistency can be preserved by periodic replacement of fouled sensors. Further, because the sensor films can be electroassembled *in situ* and used for assessing a variety of molecular species [36–42], we have developed criteria for their design. Here, protocols are developed for assays that utilize enzymes and substrates. We note that although this study focuses on a cytotoxicity assay, the concept of modularity and the design attributes described can be extrapolated to broader studies and applications.

2. Materials and methods

2.1. Device fabrication

All microfluidic devices were created using standard soft lithography methods in the Maryland Micro and Nano Fabrication Center. Device designs were modelled on AutoCAD (Autodesk, Inc., Mill Valley, CA) and developed as a Mylar mask. SU-8 3050 photoresist (MicroChem, Westborough, MA) was deposited onto a sterilized 4 inch diameter silicon wafer. After spinning the wafer for 45 s at 2600 rpm, the wafer and photoresist were soft-baked at 95 °C for 15 min. The Mylar mask was aligned with the wafer to transfer the design onto the photoresist through UV light exposure (405 nm wavelength) using an EVG 620 mask aligner (Electronic Visions Inc., Phoenix, AZ) at an exposure energy of 23.4 mW cm^{-2}. After undergoing a post-exposure bake of 95 °C for 20 min, the wafer was submerged and agitated within SU-8 developer (MicroChem) for 8 min to create the final master structures. Isopropanol and deionized (DI) water was used to wash away residual photoresist.

The microchannel layer was made from polydimethylsiloxane (PDMS) (Sylgard 184, Dow Corning Co., Midland, MI) cast on an SU-8 master. PDMS was prepared by mixing the polymer material and curing agent (10:1 w/w) and deposited on the master structures followed by baking at 60 °C for 1 h. Upon PDMS delamination from the mold, a 1 mm biopsy punch (Miltex, York, PA) created inlets and outlets. Cell culture devices were created by subjecting a PDMS layer and 30 mm glass coverslip (Bioptechs Inc., Butler, PA) with oxygen plasma using March Plasmod oxygen plasma cleaning system (Nordson Plasma Systems, Concord, CA). Microfluidic mixers were created in a similar fashion but used PDMS as the base layer instead of a glass surface. The base layer for the sensor contains a pattern of three-electrode system that was custom designed on AutoCAD, converted, exposed, and developed onto a stainless-steel shadow mask. The pattern was transferred from the mask to circular glass coverslips by depositing 5 µm chromium and 50 µm **gold** sequentially using Metra Thermal Evaporator (Telemark, Battle Ground, WA). Sensors were fabricated by bonding the PDMS channel layer to the base layer with proper alignment. The sensor was equipped with a holder and rod electrodes for a simple and stable connection to the external electrical source. Both sensor holder and modular chip holder were designed using Solidwork (Dassault System, Velizy-Villacoublay, France) and 3D printed by a Connex 3 Object500 and MED610 in. (Stratasys, Eden Prairie, MN).

2.2. Preparation of "molectronic" sensor with bio-based redox capacitor (BBRC) films

The sensors were functionalized with BBRC films in two steps [2,3,38,39,43]. First, the target working electrode was connected to an external electrical power supply (2400 Sourcemeter, Keithley, Cleveland, OH) and set as the cathode. A nearby electrode was set as the anode. The microchannel (3 mm x 3 mm x100 μm) was filled with 1.1% chitosan solution (Sigma-Aldrich, St. Louis, MO) to immerse both electrodes. A constant current of 3 A/m^2 was applied for 30 s to selectively electrodeposite chitosan film (~ 50 μm thick [44]) on the cathode. Second, the device was connected to a potentiostat for catechol grafting. The channel was filled with catechol solution (5 mM, pH 7.0) (Sigma-Aldrich), and a constant anodic potential of +0.6 V (vs Au) was applied for 3 min to oxidize the catechol. The oxidized catechol (*i.e.*, o-quinone) undergoes grafting reactions to the chitosan film ([38,39,23,45],). In order to confirm the signal amplification capabilities of the film, the channel was filled with 50 μM 1,1'Ferrocenedimethanol (Fc) (Acros Organics, New Jersey, NJ) and 50 μM hexaammineruthenium chloride (Ru^{3+}) (Sigma-Aldrich, St. Louis, MO) in phosphate buffer (PB) (pH 7.0). Chronocoulometry (CC, 0.5 V, 120 s) was applied to electrochemically charge and discharge BBRC films. Films at fully charged and fully discharged states were generated by the electrochemical redox-cycling reactions. The resulting sensor is named as "molectronic" (*i.e.*, molecular to electronic) sensor.

2.3. Modular system dynamical characterization

The system was assembled by connecting the OOC, the mixer and the molectronic sensor sequentially via microtubings as depicted in Fig. 1**A**. The mixer was connected to both the OOC and a syringe filled with substrate solution for LDH catalyzed reaction (*i.e.*, 20 mM L-lactate (Sigma-Aldrich), 10 mM β-nicotinamide adenine dinucleotide sodium salt (NAD+, Sigma-Aldrich), 50 μM Fc in PB). The system was driven by syringe pumps (Kent Scientific, Genie Plus; Fisher Scientific, Single Syringe Pump) propelling PB and LDH substrate at flow rates of 30 μl/hr and 270 μl/hr, respectively. To examine the fluidic dynamics in the system (mainly from OOC to sensor), Fc was used as an electrochemical tracer. Fc (500 μM in PB) was manually introduced into the cell-on-a-chip as a sample. At time zero, the device was plugged into the system (Fig. 1A) when time was set as t_0. A constant chronoamperometry (CA) was applied to monitor Fc concentration in the molectronic sensor. In parallel, fluid dynamics and finite element simulation were respectively modeled using MATLAB software (The MathWorks, Natick, MA) and Comsol Multiphysics (COMSOL Inc., Stockholm, Sweden). In MATLAB, the axial dispersion model was applied based on Fick's law ($\partial C/\partial t = D \times \partial^2 C/\partial x^2$, D = diffusion coefficient). The minimal lengths for both the mixer and the connecting tubings (extender) between the mixer and the sensor were calculated to accommodate the mixing molecules with different diffusion coefficients and enzymatic kinetics. The detection limit of the sensor was the background noise level plus three times of standard deviation (σ). The minimal extender length is modeled based on equation L= ((143.7 − 16.5 × x)/x) × 33.3, where L is the minimal length of the extender for the LDH reaction to generator a minimal signal (143.7 μM of NADH), x is the maximal reaction rate (V_{max}) of LDH and 33.3 is the flow speed in unit of mm s^{-1}.

2.4. On-chip cell culture

The model cell line used in this study was Caco-2 cells obtained from American Type Culture Collection (Manassas, VA). Cells were maintained using Dulbecco's Modified Eagle Media (DMEM) (Gibco, Grand Island NY) supplied with 10% fetal bovine serum (FBS) and 1% pen-strep antibiotic (Gibco) in T75 flasks under 37 °C and 5% CO_2 level and passaged every three days. The devices were sterilized with 70% (v/v) ethanol and 30 min of UV light exposure before cell introduction. Sterilized channels were coated with 50 μg/ml type I collagen and 300 μg/ml Matrigel matrix (Corning, Corning, NY) at 37 °C for 2 h. Caco-2 cells were then gently transferred to the device using 1 ml syringes at approximately 1.5 × 10^5 cells/cm^2/ml. Once the inlets and the outlets have been sealed, the device was incubated at 37 °C in 5% CO_2 for 1 h to allow cells to attach to the substrate. Then, culture media was perfused through the channel at a constant flow rate of 30 μl/hr to replenish nutrients. The entire culture system was incubated at 37 °C in

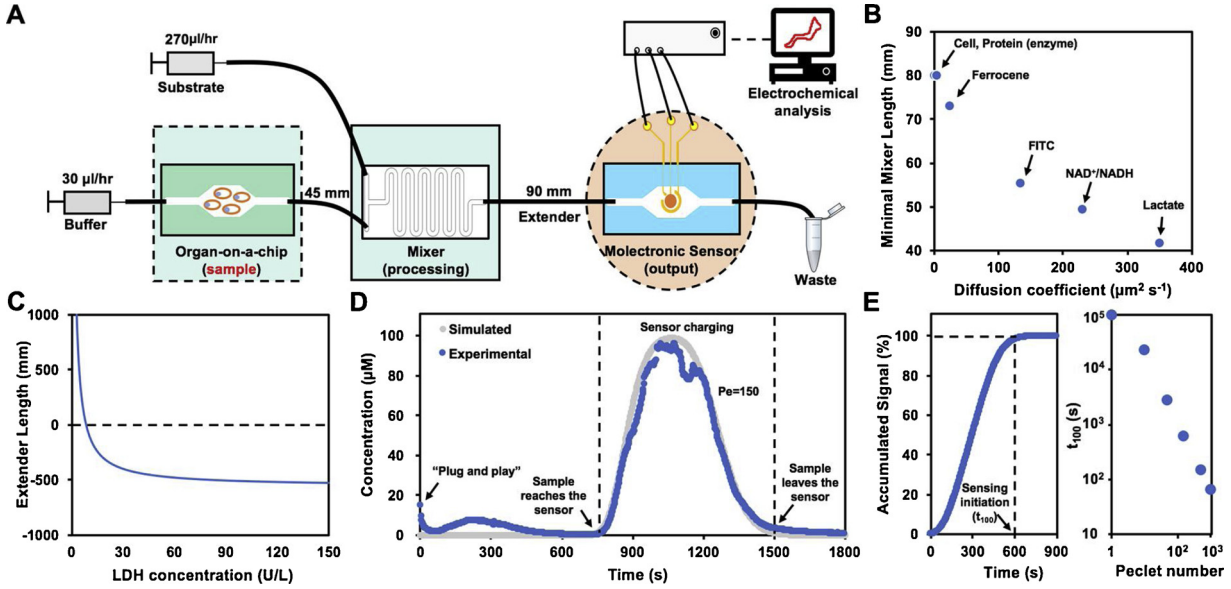

Fig. 1. Design and characterization of the modular system. (A) Schematic diagram of the modular assay system. (B) Calculated minimum length of the mixer required for analytes of various diffusion coefficient to reach homogenous mixing. The diffusion coefficient of the enzyme (*e.g.*, LDH) is at least one order of magnitude less than chemicals in the substrate solution and is neglected during mixing. (C) Calculated length of the extender required to generate a minimum NADH signal (background + 3σ) for samples with various levels of LDH (*e.g.*, rates of enzymatic reaction). (D) Concentration profile of model analyte (Fc) as it progresses from the OOC through the mixer and into the sensor module. This is overlaid with the predicted quantities for Pe = 150. (E) Predicted signal accumulation in the sensor module after the sample reaches the sensor (left). Time required to reach 100% signal accumulation (t_{100}) for systems as a function of Peclet number (right).

5% CO_2 for 24 h before experiment. The viability of each culture was assayed and visualized with a LIVE-DEAD viability/cytotoxicity kit (Thermo Fisher Scientific, Waltham, MA) and the molectronic sensor.

2.5. Microfluidic mixer characterization

The mixer was characterized using 1.5×10^{-5} M fluorescein isothiocyanate (FITC) (Thermo Fisher Scientific, Rockville, MD). This method was based on the observation that the intensity of fluorescence emission from fluorescein solutions in a microfluidic channel (depth 100 μm) was linearly proportional to the fluorescein concentration (not shown). This linearity held when the fluorescein concentration was less than 10^{-3} M. [46] FITC and deionized (DI) water were introduced into the mixer at flow rates of 30 μl/hr and 270 μl/hr, respectively. At steady state, fluorescence images were taken using a CCD camera, an inverted fluorescence microscope, a FITC filter cube, and a 10X Olympus objective lens. Fluorescence intensity was analyzed using ImageJ (shareware: https://imagej.nih.gov/ij/) and normalized to the fluorescent intensity at the inlet.

2.6. Cytotoxicity testing

To chemically disturb cell cultures in microfluidic devices, a drug mimic, Triton X-100 was used. Triton X-100 was diluted in DMEM and pumped into devices at 40 μl/hr for 3 min. Then, the outlets were sealed to stop the flow and the device was incubated at 37 °C for 2 h. After the incubation, the cell culture modules were "plugged" into the cytotoxicity testbed (*i.e.*, the inlet and the outlet were connected to a syringe and the mixer, respectively). Time was set as t_0 when the device was plugged in. Based on the system characterization demonstrated in Fig. 1D, the molectronic sensor starts to discharge at t = 4 min. The BBRC was fully discharged (*i.e.*, no further change in CC, the film's catechols were all in oxidized = O form) at t = 12 min. Then, a 10-minute sensor charging was set to allow the BBRC films being enzymatically charged (*i.e.*, the film's quinones were converted to catechols) by NADHs produced through LDH catalyzed reactions. At t = 22 min, CC was applied to measure the electrons accepted and stored in the BBCR films. Based on the in vitro assays and data from previous work, cells treated with 0.1% of Triton X-100 were set as the positive controls. Cell-less DMEM with and without 0.1% Triton X-100 addition were set as the negative controls. The cytotoxicity of each sample was calculated using Eq. (1):

$$\text{Cytotoxicity}\,(\%) = [\text{LDH}]/[\text{LDH}]_{\text{Max}} \times 100\%, \quad (1)$$

Where [LDH] referred to the normalized LDH level measured in each sample and $[\text{LDH}]_{\text{Max}}$ referred to the normalized LDH level in the positive control. All [LDH] were normalized by subtracting the negative controls. For standard curve preparations, LDH stock solutions were spiked into the substrate solution to make samples with LDH concentrations of 0 unit/L, 15 unit/L, 30 unit/L, 45 unit/L, 60 unit/L, 90 unit/L and 120 unit/L (1 unit of LDH produces 1 μmol of NADH in 1 min). After each experiment, the system was thoroughly washed with PB.

2.7. Long-term cell culture and quality control (QC)

To evaluation sensor stability during a long-term experiment, quality control (QC) units were connected to the mixer in replacement of the model OOC. The QC units have the same configuration as the model OOC but contain sensor characterization solution (50 μM Fc/Ru^{3+} in 0.1 M PB, pH 7.0) instead of cell culture. The sensor characterization solution was used to test the maximal capacitance of the films (*i.e.*, charging the film with excess Ru^{3+} followed by titrating the film with excess Fc). Such measurement was conducted between every cytotoxicity testing. To examine the effect of different factors on sensor fouling, an array of sensors was treated under various conditions (*e.g.*, constant flow, exposure to biological components) and their maximal capacitances were compared between day 3 and day 1.

A five-day experiment initiated with two OOCs incubated simultaneously at 37 °C in 5% CO_2 with continuous perfusion of warm DMEM at a flow rate of 30 μl/hr. After every 24 h, cells were treated with 0.1% Triton X-100 followed by cytotoxicity testing. This experiment was repeated for five days. The cytotoxicity testing was conducted using two groups of sensors: 1) daily made fresh sensors ("modular"); and 2) reused sensors that were incubated with the OOCs ("built-in"). Cytotoxicity was calculated using Eq. (1), except $[\text{LDH}]_{\text{max}}$ referred to the LDH level measured in day 1.

In general, because we have created the microfluidic and microelectronic systems using standard lithographic methods (*e.g.*, PDMS, glass, *etc.*), we expect these components to be reusable for many cycles. Because sensing components (*e.g.*, catechol-modified chitosan, proteins, *etc.*) are electronically assembled *in situ*, they are easily assembled, used, and "erased" (acid washed) as needed [47–50]. That said, repeated use of the catechol-modified film was observed to be stable over a 77 day sampling period for a different study using human sera [35].

2.8. Instrumentation

All electrochemical measurements were performed using a CHI 6002e electrochemical analyzer (CH instruments, Austin, TX). Caco-2 cell cultures were imaged using a fluorescence microscopy (BX 60 microscope; Olympus) and a digital camera (Olympus DP72).

2.9. Statistical analysis

All assays were performed in triplicate. Results were expressed as mean ± standard error. One-way ANOVA was used to determine significant differences between groups. The level of significance was set at $\alpha = 0.05$. The Pearson product-moment correlation coefficient was applied to measure the strength of linear correlation between groups. The level of significant correlation was set at $r = 0.95$.

3. Results and discussion

3.1. Modular assembly – design and characterization

The modular system demonstrated here consists of four components: an OOC (2D on-chip cell culture) and three accessorial modular units including: (i) a mixer wherein the OOC sample effluent is mixed with substrate and converted to an assayed biomarker; (ii) a "molecular-electronic (molectronic)" sensor that measures the biomarker quantity electrochemically; and (iii) a quality control (QC) module (see Scheme 1) that replaces the OOC to monitor sensor function. Each module is connected via microfluidic tubing wherein length is a design parameter; the system is controlled via syringe pumps and programmable electronics. Since the concept of modularity is envisioned to be generalizable for expanded OOC application, fluidic and enzymatic kinetic analyses were conducted. These provide criteria for designing critical dimensions of the system. For example, the length of the mixer is designed according to the criteria that homogeneous mixing between sample and substrate be achieved by its exit port.

Fig. 1A shows the configured device for this application. Because the measure of cytotoxicity is determined by the quantified activity of released lactate dehydrogenase (LDH), its level is determined by the outcome of an on-chip enzymatic reaction. Owing to laminar flows prevalent in microfluidics systems, mixers that rely on molecular diffusion of analytes across adjacent streams provide the requisite residence times for enzymatic reactions to proceed. Recognizing that the length of the mixer is a function of the enzyme activity, substrate concentration, and fluid flow rate, we performed a modeling analysis to calculate the minimum distance (hence time) needed to determine the analyte level needed for its assessment within the sensor chip. These

enzyme/flow methodologies are general and can be used for potentially any on-chip enzyme assay, but they are demonstrated here for LDH. Fig. 1B plots the minimum length of the mixer as a function of the important diffusion coefficients – those of enzyme and the small molecule substrates. The mixer in this study was designed (length = 80 mm) to accommodate all substrates and analytes used in this study (*e.g.*, lactate, LDH, NADH).

In our Supporting Information, we performed finite element simulations of the mixer and compared these to flow experiments using fluorescein isothiocyanate. We expected and found that by the end of the mixer, the solutions were homogeneous and could be quantified via a dilution factor representing the overall dilution of the original solution (Fig. S1B–D, Supporting information). As noted, the length of the extender (distance between the mixer outlet and the sensor inlet) was designed based on the criteria that a requisite minimum signal (*i.e.*, background + 3σ) is generated as the sample reaches the sensor. In other words, the extender provides increased time for reaction, if needed, beyond that of the mixer. Considering OOC samples with different initial enzyme concentrations yield distinct enzymatic kinetics within the mixer (Fig. S2, Supporting Information), the extender length profile can thus be adjusted accordingly (Fig. 1C). Theoretically, an infinitely long extender is required for a sample with infinitely small enzyme activity. It should be noted that as enzyme activity increases, the required length for the extender becomes negative; the minimal signal is actually generated before the solution leaves the mixer. For instantaneous reactions, the extender length is defined by the diffusivity and flow rate. That is, the total reaction time needed is given by the point in the mixer where 100% of the OOC effluent is mixed with the reactants. The extender used in this study (90 mm) ensures that the enzymatic reaction was sufficient for all samples (LDH released from the positive control group (*e.g.*, dead cells) is 27.8 unit/L).

The fluid dynamics of the modular system, including the mixer, extender, and molectronic sensor, were first characterized using 1,1'Ferrocenedimethanol (Fc), an electrochemical mediator as a control that is easily quantified as current following an applied voltage on the electrode in the floor of the sensor chamber. Fc solution (500 μM in PB) was introduced to the OOC as a bolus and flowed downstream (30 μl/hr) through a mixer and a sensor. Chronoamperometry (CA) was continuously applied within the sensor module to monitor the prevailing Fc concentration. An LDH assay substrate solution (*i.e.*, 20 mM L-lactate, 10 mM NAD + and 50 μM Fc in PB) was also continuously introduced to the mixer at a flow rate of 270 μl/hr using a second fluid port as a mock assay control. The entire system was operated under continuous flow. That is, we held the extender flow steady at 300 □l/hr until 12 min when the Fc solution was replaced by PB. Fig. 1D represents the concentration profile of Fc measured within the sensor (converted from the measured current and normalized to 100). The measured Fc levels matched our expectation (the final Fc concentration is a combination of 10 times diluted effluent from the OOC and 9/10 times diluted substrate). The result illustrates that after system assembly (t = 0 min), sample (Fc) reached the sensor at t = 13 min and had completely exited by t = 25 min. The concentration profile was compared to a plug flow reactor with axial dispersion. We matched the experimental results with the model and found the best fit Peclet number (ratio of convective to dispersive flow) to characterize the system (Pe = 150). This high value demonstrates that the flow in the fluidic channels was near ideal and with minimal axial dispersion.

During testing with media and LDH (marker of cytotoxicity), signal (NADH) is first accumulated in the sensor (*i.e.*, sensor charging) before the sample is measured. The level of accumulated signal is proportional to original biomarker concentration (*i.e.*, NADH, biological reductant) in the sample. Accumulated signal was plotted as a function of time by calculating the area under the concentration profile curve in Fig. 1D and E). In this figure, the x axis was normalized to the time when the sensor charging begins (*i.e.*, t = 13 min) or, in general, when the sample reaction mixture first leaves the extender. It should be noted that although enzymatic reaction initiates as soon as samples interact within the mixer, the product (NADH) has a relatively low decomposition rate (6% per hour [51]) and can still be accumulatively measured at the sensor (for the entire duration of the assay −22 min). According to our simulations, a minimum of 10 min of charging (t_{100}, or the time to a 100% signal - see the arrow in the left panel of Fig. 1E) was needed to ensure a sufficient signal (˜100%) is detected. Interestingly, we found that t_{100} was linearly dependent on Peclet number in the fluidic system, suggesting that charging time can be adjusted according to fluidic dynamics.

In this example, we show how the enzymatic reaction and the fluid flow rates are coordinated; these processes must be modeled so that system modularity can be optimized. We note further that these simulations are not difficult and the processes described here can potentially be used for any enzyme/substrate assays (*e.g.*, glucose [52]). They are likely not necessary for assays with analytes having redox properties (*e.g.*, Fc, pyocyanin [43,53]).

3.2. Molecular information access from organ-on-chips - cytotoxicity testing using a "molectronic" sensor

While the basis for the design was demonstrated in Fig. 1, in Fig. 2 we show the specific results for an LDH-based cytotoxicity assay. That is, we employed a cytotoxicity assay to demonstrate the concept of microchip modularity so that biological molecular information access can be facilitated from OOCs using electrochemical sensors that are assembled and employed *in situ*. In this figure, we also demonstrate "plug and play" modularity for OOC systems. A simple 2D OOC was constructed that contained a culture chamber (3 mm x 3 mm x100 μm) flanked by two channels connecting both an inlet and an outlet (Fig. 2A). A human epithelial colorectal adenocarcinoma cell line, Caco-2, was used as a model cell culture. Caco-2 cells are commonly used in drug delivery studies involving transport through the enterocytes lining the human small intestine ([54] [55];). Caco-2 cells (1.5×10^5 cells/cm^2/ml) were gently introduced into the OOC system using syringes. After 1 h (cells attached to the substrate), pre-warmed DMEM (with 10% FBS) was perfused through the channel at a constant flow rate of 30 μl/hr (which produces 0.02 dyn/cm^2 shear stress [2,3]) for 24 h before the experiment. The entire cell culture system was incubated at 37 °C in 5% CO_2. In Fig. 2A, Caco-2 cell cultures are shown using microscopy (bright-field and fluorescence). We used a fluorescence based viability kit in end-of-experiment samples to demonstrate highly viable cells as model inputs. Caco-2 cells were cultivated in oxygenated DMEM at 37 °C for 24 h in a perfusion mode with a flow rate of 30 μl/hr. In Fig. 2A and B, "sample" refers to the supernatants exiting the OOC. That is, upon cell membrane damage, an enzymatic biomarker, lactate dehydrogenase (LDH), is released from cell cytosol to the surrounding environment. This solution, containing LDH, is added in parallel to the substrate solution, and both are flowed downstream through the mixer and then sensor modules. The LDH level here is a surrogate for the cytotoxicity of applied drugs or other factors [56,57,58].

The sensor module used in this work is a "molectronic" sensor developed by our group (Fig. 2B) [41]. A key part of the molectronic sensor is that its working electrode is functionalized with an electro-assembled catechol-modified chitosan film. That is, it is assembled *in situ* by a simple biasing of an electrode embedded within a device under or along the sidewall of a microfluidic channel, creating a basic solution in the direct vicinity of the electrode. Chitosan and catechol-modified chitosan, which have pH-dependent solubility, form thin films or hydrogels that adhere directly on the electrode surfaces depending on the applied charge [59,60]. Once assembled, this film can then store charge for extended periods and also "write" charge under an applied voltage, we have referred to these films as bio-based redox capacitors (BBRC) [2,3,38,39]. That is, BBRC films are non-conducting (*i.e.*, unable to exchange electrons directly with the underlying electrodes) but they are redox-active and can repeatedly exchange (*i.e.*, accept, store and

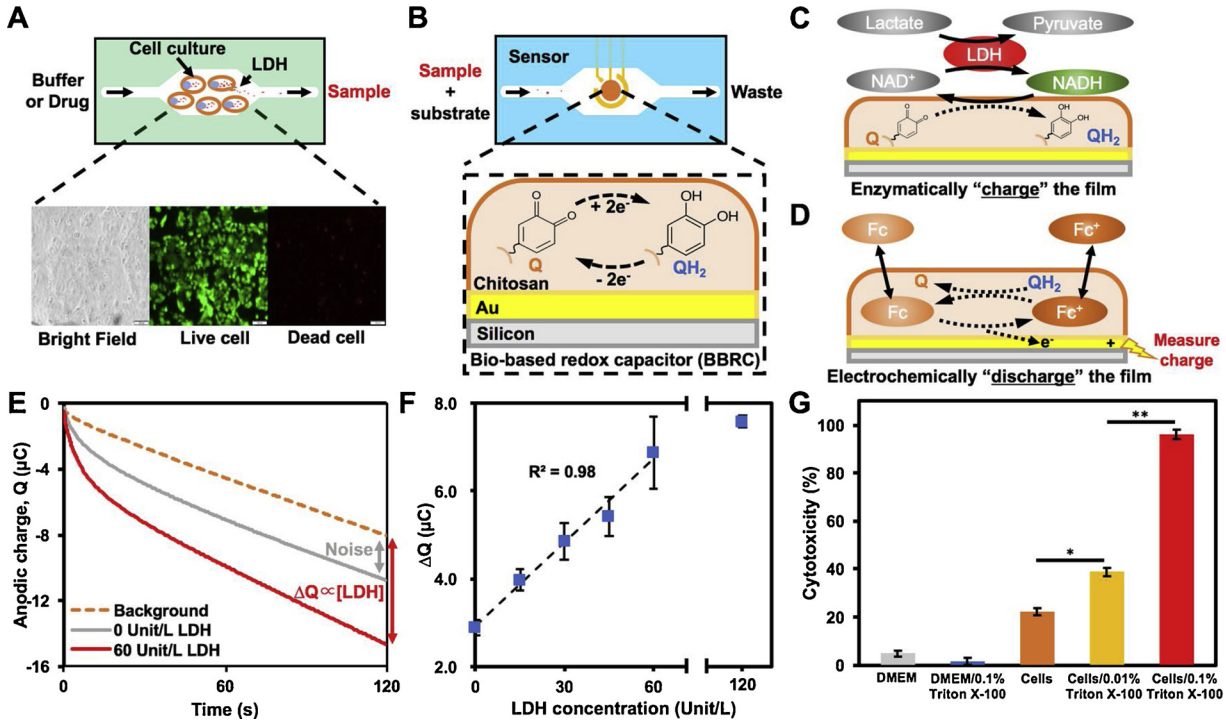

Fig. 2. Accessing molecular information from organ-on-chips (OOCs). (A) Schematic of an OOC module comprised of human intestinal epithelial cells, Caco-2 cells, grown in DMEM. Sample (culture supernatant) is pumped downstream after fluidically connecting to mixer and sensor modules. Microscopic images taken after 24-hr culture indicate coverage and viability (> 90%). Scale bar = 100 μm. (B) Schematic of molectronic sensor module. Catechol is conjugated to an electro-assembled chitosan film. The redox state of the quinone/catechol can be modulated using redox mediators and applied voltage. The catechol-modified chitosan is referred to as a bio-based redox capacitor (BBRC) owing to its ability to store and exchange electrons. (C) Lactate dehydrogenase (LDH) converts lactate (substrate) and NAD^+ (cofactor) to pyruvate and NADH, which, in turn, donates electrons to the quinone moieties in the BBRC film (*i.e.*, enzymatic charging). (D) Oxidative redox-cycling between Fc^+/Fc and the BBRC film. Using this method, electrons stored in the BBRC film can be "titrated" and quantified as "charge" (current x time). (E) Chronocoulometry results comparing an LDH-spiked sample (with the substrate in PB) to the negative control (film incubated with the solution without LDH). The dotted line represents the background where the film is fully discharged using the Fc-oxidative cycling. (F) LDH activity titrated as charge in the sensor module. (G) Normalized cytotoxicity measurements on OOCs with various treatments (**, $p < 0.01$; *, $p < 0.05$). Q: quinone; QH_2: Catechol.

donate) electrons with soluble redox-active species, those either from the biological systems under study or added to the systems to infer biological information. Soluble biological reductants (*e.g.*, NADH) can donate electrons to the BBRC films through a reductive-redox cycling (converting quinone (Q) to catechol (QH_2)), which is also known as "enzymatic film charging" (Fig. 2C). The electrons stored in the charged film can then be "titrated" (*i.e.*, extracted) by an oxidative-redox cycling using Fc as a mediator (Fig. 2D). We show that through redox cycling, more electrons can be titrated from fully charged films (the film's catechols all originally stored in the reduced QH_2 form), compared with fully discharged films (the film's catechols are all in the oxidized Q form) (Fig. S3, Supporting Information). Hence, through redox cycling significant signal amplification is achieved.

To measure the cytotoxicity level of the cells within the OCC, the molectronic sensor module was connected to the outlet of the mixer module in the fluidic system. Importantly, the sensor module is easily fabricated and easily changed for simple use. Before every test, the sensor was fully discharged to the background level corresponding to all catechol moieties in the oxidized Q form. The OOC module was connected to the inlet of the mixer and sample was assayed according to the protocol described in Fig. 1. That is, in addition to the OOC outlet flow being introduced to the mixer, by introducing excess lactate and NAD^+ as substrates at defined rates in the second feed to the mixer module, the LDH activity is assayed by the generation of NADH. In the sensor module, chronocoulometry was then employed to quantify titrated charge. In Fig. 2E, the fully discharged BBRC film (the dotted line) was incubated with various solutions with no applied voltage and then each resulting film was titrated by the Fc-redox cycling reaction. Compared to the control group where the film was incubated in solutions lacking LDH (the grey line), the red line indicates a large oxidative charge was generated from a mixture of LDH spiked sample and substrates that were allowed to react as they flowed through the mixer and extender. These results confirmed that the products from LDH catalyzed reaction (*e.g.*, NADH) charge the BBRC film enabling signal measurement upon oxidative discharging. The magnitude of the signal is dependent on the number of reduced catechols in the film, which, in turn, are linearly proportional to prevailing the LDH concentration (Fig. 2F). Importantly, the response was found to be linear up to 60 unit/L, where the signal appeared to saturate. This observed signal saturation was presumably due to the limited contact efficiency (confined space for diffusion) between NADH in the bulk solution and the film within microchannel [61]. This size-based limitation could be relieved by either increasing the electrode size or by depositing more catechol-modified chitosan onto the electrode. In the latter case, this demonstrates the ease by which modifications can be made using this methodology. By applying voltage for a longer time one controls the period of electroassembly, so that more chitosan can be deposited increasing the number of catechols in the BBRC.

Using molectronic sensors, cytotoxicity levels of chemically-disturbed OOCs were measured. All results were normalized to the positive control (cells treated with 0.1% Triton X-100 are ~17% viable [62], however in our case, the viability was near 0% [41]) and the negative control (cell-free DMEM media). Results in Fig. 2G corresponded with our expectations that cells treated with the drug mimics (Triton X-100) yielded a significantly higher cytotoxicity level ($p = 0.016$) than that was otherwise observed for healthy cells. Moreover, increased Triton X-100 resulted in increased cell death ($p = 0.001$). We also note that the negative mimic case with cells and no drug did exhibit a nonzero level

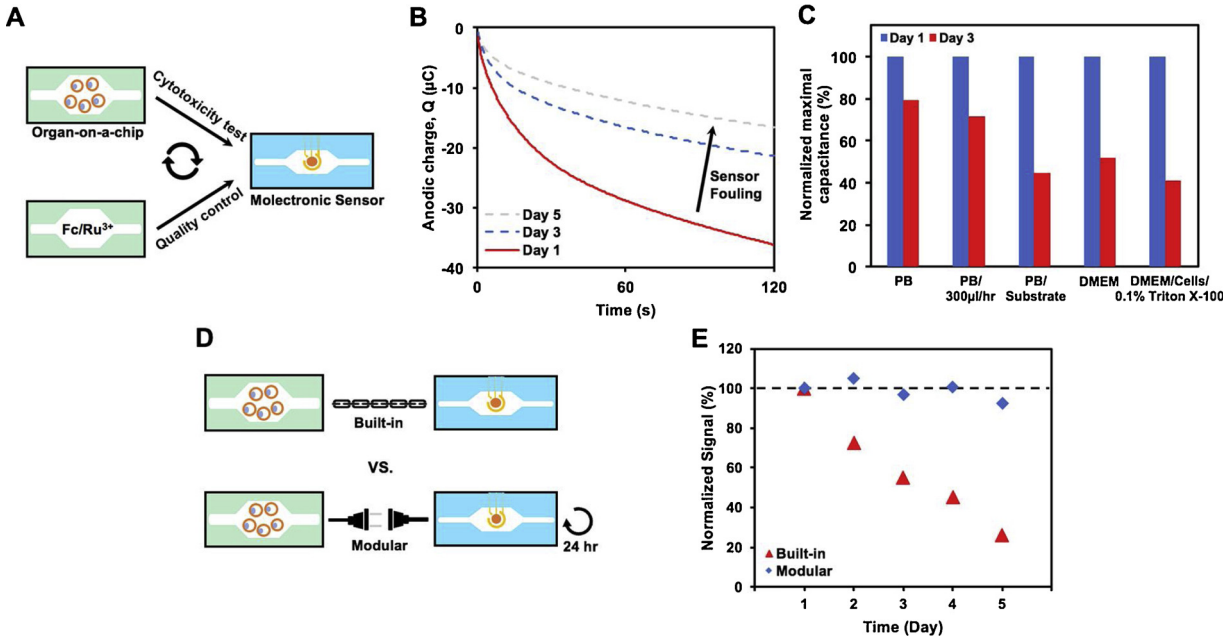

Fig. 3. Introduction of a quality control (QC) module. (A) Conceptual scheme of QC module for sensor evaluation. The QC module is exchanged with OOC to conduct sensor quality control. (B) The quality of sensor module was controlled by measuring the maximal signal amplification capacity (fully charged by the Ru^{3+}-reductive cycling followed by titration using the Fc-redox cycling reaction) of the BBRC film within microchannel. Chronocoulometry results of a molectronic sensor at day 1, 3, and 5 were compared. Day 1 is the first day that the sensor is made. The sensor is reused and stored at 37 °C and 5% CO_2. (C) An array of devices was treated in various ways to examine the potential cause of sensor fouling. For each group, measured signals from day 3 were normalized to results from day 1. (D) Conceptual scheme illustrating long-term "built-in" OOC/sensor modules (upper) and a "modular" assembly (lower) format. (E) Systems assembled with both "built-in" and "modular" formats were used to measure the cytotoxicity level of OOCs for five days. For both systems, measured signals from day 2 to day 5 were normalized to results from day 1 to compare assay consistency.

of cytotoxicity, indicating some partial release of LDH and activity above the enzyme-free controls.

Overall, these data demonstrate that appropriate placement of functional modules (*e.g.*, sensor and mixer) enable the rapid assessment of cytotoxicity in OOC systems. Most importantly, the *in-situ* measurements showed here, are quantitative and require no pooling of sample (essential for samples with volume at sub-microliter scale) and are essentially real-time. Should sensors require changing, new chips can be reassembled in minutes and used for replacement. In this way, labile components can be stored appropriately offline and brought into the system as needed.

3.3. Introduction of a quality control (QC) module

One deficiency associated with current built-in sensors in OOCs is the lack of quality control monitoring of sensor and mixer function during long-term cell cultures. For example, repeated exposure to cell culture media increases the chance of sensor fouling, which, in turn, leads to assay inconsistency. We developed modular QC units that contained control solutions (50 μM Fc/Ru^{3+} in 0.1 M PB, pH 7.0) for monitoring sensor function (Fig. 3A). In this configuration, the QC module replaces the model OOC between cytotoxicity tests and enables continued examination of the signal amplification capacity of the BBRC film housed within the sensor module. Briefly, the BBRC film was electrochemically charged to its fully charged state using the Ru^{3+}-reductive cycling (*i.e.*, maximal capacity). The charging state of the film was then titrated and measured by the Fc-redox cycling reaction. A daily decrease in maximal film capacity was observed over the course of a five-day experiment (Fig. 3B, data for days 2 and 4 not shown). This drop was presumably due to either the loss of catechol from BBRC films under a constant flow, or more likely, the fouling of BBRC films upon repeated contact with complex culture media, cell debris and substrate solution (exacerbated in miniaturized device) (Fig. 3C) [35].

We tested whether the decrease in maximal film capacity would lead to a decrease in cytotoxicity measurement consistency (Fig. 3D). For this, we created a long-term exposure test and a plug-and-play modular format. In the long-term format denoted "built-in", a single sensor was incubated with an array of five OOCs at 37 °C and 5% CO_2 for five days. On each day, one OOC was chemically treated followed by a cytotoxicity test. All tests in five days were conducted using the same "built-in" sensor. In the "modular" format, sensor function was monitored between assays and fouled sensors were replaced (typically within 24 h) (Fig. 3D). For every measurement, cells in OOCs were cultured and treated (0.1% Triton X-100 in DMEM) in the same manner. In the "modular" format, sensors renewed daily yielded nearly identical results with a variation of less than 10% (Fig. 3E). This indicates both assay consistency and relative uniformity in the assembly process. By contrast, the measured value of cytotoxicity by the "built-in" sensor showed a consistent drop, which was in accordance to the aforementioned decrease in BBRC film capacity. Signals measured from these two groups showed significant differences ($r = 0.603$, $p = 0.015$) even with similar inputs. In sum, our studies suggest that modularity enables us to monitor sensor function and thus maintain assay consistency by adding or replacing modules during long-term experiments.

4. Discussion

Many organ-on-chips (OOCs) utilize optically transparent microfluidic systems so that fluorophores, including those conjugated to antibodies and receptors that fluoresce based on functional or biophysical microenvironments (pH, oxygen level, *etc.*), can be imaged enabling functional information from within the device. Ancillary MS or LS/MS and other omics-based instruments augment fluorescence data, and while vitally important, these are often end-of-experiment measures from pooled samples and they are typically not in real time. We have developed a methodology for electro-addressed sensors that provide easily accessed molecular information in near real time.

In the present work, we show how various modules including a new

quality control (QC) module, when assembled and incorporated into the modular system, can provide accurate molecular information in near real time and for extended periods of time. Modules, including the main cell culture chip, can be assembled and dissembled based on their function and design characteristics (rapidly assembled sensors, slowly assembled OOC, mixer, *etc*.). Such modular assembly vastly expands our capability to analyze/manipulate samples within miniaturized structures while keeping OOCs in their original designs. The entire process is hands-free after assembly. By controlling fluidics, the modular system prevents unwanted interaction between modules (*e.g.*, deleterious biorecognition components affecting cell cultures). That is, the flexibility enabled by modularity permits all modules to be prepared on demand and, in turn, designed in such a way so as to avoid many problematic issues pertaining to OOC design and use. Integrated sensors, for example, can present challenges due to fouling and the decay of biorecognition elements (*e.g.*, antibodies, receptors, enzymes). Moreover, it is difficult to fabricate OOCs with embedded biological recognition elements owing to their labile nature and the various lithographic or additive manufacturing assembly methods. Electroassembly methodologies, as described here, require minimal instrumentation and can be performed in common laboratory settings at the time of use.

We demonstrate a proof-of-concept study by conducting cytotoxicity measurements on model OOCs (GI epithelial cell cultures) using an interconnected microfluidic device consisting of mixers and redox-based molecular electronic “molectronic” sensors. These sensors are assembled *in situ* and because they rely on internal reference measurements, are highly accurate. Moreover, they can be comprised of labile biological components (*e.g.*, polysaccharides and proteins) as they are assembled in minutes directly onto electrodes via applied voltage. There are no harsh chemicals or mechanical systems. Importantly, we additionally show how quality control modules could be designed to monitor sensor function. We use them here to maintain assay consistency by replacing fouled sensors. Accordingly, their use could likely be extended for evaluating other components in the system (see Scheme 1).

We believe modularity vastly increases the “toolbox” by which investigators can design, build, and use OOC systems. Sensors, regardless of their biocompatibility and shelf-life, can be modularly incorporated into OOCs for broader information access. While we showed how one system is used to assay LDH activity, the same system can be used to assay small molecules that are detected using other enzymes – particularly those involving redox active co-factors such as NAD^+. Also, this approach can be extended to analytes that do not involve enzymatic reactions, such as other redox-active molecules (Fc, pyocyanin ([53,63,35,43,61,64–66],)) that are measured directly. Further, non-redox active molecules can be converted to redox active analytes by enzymes (*e.g.*, glucose [52], antibodies [66] or by cells (using cell-based sensors that report on small molecule detection by the expression of ▭-galactosidase [40]). Future work might incorporate controller units (*e.g.*, valves) to develop self-contained *in vitro* testbeds wherein module connection/disconnection is automated, and inputs (*e.g.*, drug stimuli, signaling molecules) and outputs (*e.g.*, cell metabolites, cell behavior) can be programmably controlled and monitored. Eventually, we envision this work provides a promising path to advance preclinical models for drug development in the biopharmaceutical industry.

Declaration of interests

☒ The authors declare that they have no known competing financial interests or personal relationships that could have appeared to influence the work reported in this paper.

☐The authors declare the following financial interests/personal relationships which may be considered as potential competing interests:

Author Credit Statement

Wu Shang was a graduate student and was involved in conceptualization, designing and executing the research (investigation), visualization, writing, and data curation.

Chen-Yu Chen is a graduate student and was involved in conceptualization, designing and executing the research (investigation), visualization, writing, and data curation.

Kimberly Lo is an undergraduate student who was involved in execution of the experiments (investigation).

Gregory F. Payne is a professor and was involved in conceptualization, resources, funding acquisition, methodology and review and editing.

William E. Bentley is a professor and was involved in conceptualization, data curation, formal analysis, funding acquisition, methodology, project administration, resources, visualization and all forms of writing.

Acknowledgements

This work was supported with funds from the National Science Foundation (DMREF #1435957, CBET#1805274, ECCS#1807604), the National Institutes of Health (R21EB024102) and the Defense Threat Reduction Agency (HDTRA1-13-0037).

Appendix A. Supplementary data

Supplementary material related to this article can be found, in the online version, at doi:https://doi.org/10.1016/j.snb.2019.05.030.

References

[1] S. Damiati, U. Kompella, S. Damiati, R. Kodzius, Microfluidic devices for drug delivery systems and drug screening, Genes (Basel). 9 (2018) 103, https://doi.org/10.3390/genes9020103.
[2] E. Kim, Y. Liu, W.E. Bentley, G.F. Payne, Redox capacitor to establish bio-device redox-connectivity, Adv. Funct. Mater. 22 (2012) 1409–1416, https://doi.org/10.1002/adfm.201101946.
[3] H.J. Kim, D. Huh, G. Hamilton, D.E. Ingber, Human gut-on-a-chip inhabited by microbial flora that experiences intestinal peristalsis-like motions and flow, Lab. Chip. 12 (2012) 2165, https://doi.org/10.1039/c2lc40074j.
[4] C. Moraes, G. Mehta, S.C. Lesher-Perez, S. Takayama, Organs-on-a-Chip: a focus on compartmentalized microdevices, Ann. Biomed. Eng. 40 (2012) 1211–1227, https://doi.org/10.1007/s10439-011-0455-6.
[5] G. Pagano, M. Ventre, M. Iannone, F. Greco, P.L. Maffettone, P.A. Netti, Optimizing design and fabrication of microfluidic devices for cell cultures: an effective approach to control cell microenvironment in three dimensions, Biomicrofluidics 8 (2014), https://doi.org/10.1063/1.4893913.
[6] J.H. Sung, M.B. Esch, J.-M. Prot, C.J. Long, A. Smith, J.J. Hickman, M.L. Shuler, Microfabricated mammalian organ systems and their integration into models of whole animals and humans, Lab Chip 13 (2013) 1201–1212, https://doi.org/10.1039/C3LC41017J.
[7] I.K. Zervantonakis, S.K. Hughes-Alford, J.L. Charest, J.S. Condeelis, F.B. Gertler, R.D. Kamm, Three-dimensional microfluidic model for tumor cell intravasation and endothelial barrier function, PNAS 109 (2012) 13515–13520, https://doi.org/10.1073/pnas.1210182109.
[8] M. Chi, B. Yi, S. Oh, D. Park, J.H. Sung, A microfluidic cell culture device (μFCCD) to culture epithelial cells with physiological and morphological properties that mimic those of the human intestine, Biomed. Microdevices 17 (2015) 58, https://doi.org/10.1007/s10544-015-9966-5.
[9] B. Zhang, M. Montgomery, M.D. Chamberlain, S. Ogawa, A. Korolj, A. Pahnke, L.A. Wells, S. Massé, J. Kim, L. Reis, A. Momen, S.S. Nunes, A.R. Wheeler, K. Nanthakumar, G. Keller, M.V. Sefton, M. Radisic, Biodegradable scaffold with built-in vasculature for organ-on-a-chip engineering and direct surgical anastomosis, Nat. Mater. 15 (2016) 669–680, https://doi.org/10.1038/NMAT4570.
[10] N.J. Douville, Y. Tung, R. Li, J.D. Wang, M.E.H. El-sayed, S. Takayama, Fabrication of two-layered channel system with embedded electrodes to measure resistance across epithelial and endothelial barriers, Anal. Chem. 82 (2010) 2505–2511.
[11] T.A. Nguyen, T. Yin, D. Reyes, G.A. Urban, Micro fluidic chip with integrated electrical cell-impedance sensing for monitoring single Cancer cell migration in three-dimensional matrixes, Anal. Chem. 85 (2013) 11068–11076, https://doi.org/10.1021/ac402761s.
[12] M. Liu, H. Shih, J. Wu, T. Weng, C. Wu, C. Lu, Y. Tung, Electrofluidic pressure sensor embedded microfluidic device: a study of endothelial cells under hydrostatic pressure and shear stress combinations, Lab Chip 13 (2013) 1743–1753, https://doi.org/10.1039/c3lc41414k.

[13] P. Shah, V. Fritz, E. Glaab, M.S. Desai, K. Greenhalgh, A. Frachet, P. Shah, C. Seguin-devaux, M. Niegowska, M. Estes, C. Ja, F. Zenhausern, P. Wilmes, A microfluidics-based in vitro model of the gastrointestinal human–microbe interface, Nat. Commun. 7 (2016) 11535, https://doi.org/10.1038/ncomms11535.
[14] D. Bavli, S. Prill, E. Ezra, G. Levy, M. Cohen, M. Vinken, J. Vanfleteren, Real-time monitoring of metabolic function in liver-on- chip microdevices tracks the dynamics of mitochondrial dysfunction, PNAS 113 (2016) E2231–2240, https://doi.org/10.1073/pnas.1522556113.
[15] S.E. Eklund, R.G. Thompson, R.M. Snider, C.K. Carney, D.W. Wright, J. Wikswo, D.E. Cliffel, Metabolic discrimination of select list agents by monitoring cellular responses in a multianalyte microphysiometer, Sensors 9 (2009) 2117–2133, https://doi.org/10.3390/s90302117.
[16] J. Kieninger, K. Aravindalochanan, J.A. Sandvik, E.O. Pettersen, G.A. Urban, Pericellular oxygen monitoring with integrated sensor chips for reproducible cell culture experiments, Cell Prolif. 47 (2014) 180–188, https://doi.org/10.1111/j.1365-2184.2013.12089.x.
[17] E. Lima, R. Snider, R. Reiserer, J. McKenzie, D. Kimmel, S. Eklund, J. Wikswo, D. Cliffel, Multichamber multipotentiostat system for cellular microphysiometry, Sensors Actuators B Chem. 204 (2014) 536–543, https://doi.org/10.1016/j.snb.2014.07.126.Multichamber.
[18] A. Weltin, S. Hammer, F. Noor, Y. Kaminski, J. Kieninger, G.A. Urban, Biosensors and Bioelectronics Accessing 3D microtissue metabolism : lactate and oxygen monitoring in hepatocyte spheroids, Biosens. Bioelectron. 87 (2017) 941–948, https://doi.org/10.1016/j.bios.2016.07.094.
[19] A. Weltin, J. Kieninger, G.A. Urban, Microfabricated, amperometric, enzyme-based biosensors for in vivo applications, Anal. Bioanal. Chem. 408 (2016) 4503–4521, https://doi.org/10.1007/s00216-016-9420-4.
[20] A. Weltin, K. Slotwinski, J. Kieninger, I. Moser, G. Jobst, M. Wego, R. Ehret, G.A. Urban, Cell culture monitoring for drug screening and cancer research: a transparent, microfluidic, multi-sensor microsystem, Lab Chip 14 (2014) 138–146, https://doi.org/10.1039/C3LC50759A.
[21] A. Weltin, J. Kieninger, B. Enderle, A. Gellner, B. Fritsch, G.A. Urban, Polymer-based, flexible glutamate and lactate microsensors for in vivo applications, Biosens. Bioelectron. 61 (2014) 192–199, https://doi.org/10.1016/j.bios.2014.05.014.
[22] E. Kim, T.E. Winkler, C. Kitchen, M. Kang, G. Banis, W.E. Bentley, D.L. Kelly, R. Ghodssi, G.F. Payne, Redox probing for chemical information of oxidative stress, Anal. Chem. 89 (2017) 1583–1592, https://doi.org/10.1021/acs.analchem.6b03620.
[23] E. Kim, T. Gordonov, W.E. Bentley, G.F. Payne, Amplified and in situ detection of redox-active metabolite using a biobased redox capacitor, Anal. Chem. 85 (2013) 2102–2108, https://doi.org/10.1021/ac302703y.
[24] H.J. Cruz, C.C. Rosa, A.G. Oliva, Immunosensors for diagnostic applications, Parasitol. Res. 88 (2002) 4–7, https://doi.org/10.1007/s00436-001-0559-2.
[25] H. Ogi, Y. Fukunishi, H. Nagai, K. Okamoto, M. Hirao, M. Nishiyama, Nonspecific-adsorption behavior of polyethylenglycol and bovine serum albumin studied by 55-MHz wireless-electrodeless quartz crystal microbalance, Biosens. Bioelectron. 24 (2009) 3148–3152, https://doi.org/10.1016/j.bios.2009.03.035.
[26] K.J. Lampe, R.M. Namba, T.R. Silverman, K.B. Bjugstad, Impact of lactic acid on cell proliferation and free radical induced cell death in monolayer cultures of neural precursor cells, Biotechnol. Bioeng. 103 (2010) 1214–1223, https://doi.org/10.1002/bit.22352.Impact.
[27] M. Lao, D. Toth, Effects of Ammonium and Lactate on Growth and Metabolism of a recombinant chinese hamster ovary cell culture, Biotechnol. Prog. 13 (1997) 688–691.
[28] J. Li, C.L. Wong, N. Vijayasankaran, T. Hudson, A. Amanullah, Feeding lactate for CHO cell culture processes: impact on culture metabolism and performance, Biotechnol. Bioeng. 109 (2012) 1173–1186, https://doi.org/10.1002/bit.24389.
[29] T. Matsuki, T. Pédron, B. Regnault, C. Mulet, T. Hara, P.J. Sansonetti, Epithelial cell proliferation arrest induced by lactate and acetate from Lactobacillus casei and Bifidobacterium breve, PLoS One 8 (2013) 2–9, https://doi.org/10.1371/journal.pone.0063053.
[30] D. deOliveira, B. Pitanga, M. Grangeiro, R. Lima, M. Costa, S. Costa, J. Clarêncio, R. El-Bachá, Catechol cytotoxicity in vitro: induction of glioblastoma cell death by apoptosis, Hum. Exp. Toxicol. 29 (2010) 199–212, https://doi.org/10.1177/0960327109360364.
[31] N. Schweigert, A.J.B. Zehnder, R.I.L. Eggen, Chemical properties of catechols and their molecular modes of toxic action in cells, from microorganisms to mammals, Environ. Microbiol. 3 (2001) 81–91, https://doi.org/10.1046/j.1462-2920.2001.00176.x.
[32] K. Shaikh, K.S. Ryu, E.D. Goluch, J.-M. Nam, J. Liu, C.S. Thaxton, T.N. Chiesl, A.E. Barron, Y. Lu, C. Mirkin, C. Liu, A modular microfluidic architecture for integrated biochemical analysis, Proc. Natl. Acad. Sci. U. S. A. 102 (2005) 9745–9750, https://doi.org/10.1073/pnas.0504082102.
[33] C.G. Sip, N. Bhattacharjee, A. Folch, A modular cell culture device for generating arrays of gradients using stacked microfluidic flows, Biomicrofluidics 5 (2011) 022210, , https://doi.org/10.1063/1.3576931.
[34] Y.S. Zhang, J. Aleman, S.R. Shin, T. Kilic, D. Kim, S.A.M. Shaegh, S. Massa, R. Riahi, S. Chae, N. Hu, H. Avci, W. Zhang, A. Silvestri, A.S. Nezhad, A. Manbohi, F.De Ferrari, A. Polini, G. Calzone, N. Shaikh, P. Alerasool, E. Budina, J. Kang, N. Bhise, J. Ribas, A. Pourmand, A. Skardal, T. Shupe, C.E. Bishop, M.R. Dokmeci, A. Atala, A. Khademhosseini, Multisensor-integrated organs-on-chips platform for automated and continual in situ monitoring of organoid behaviors, Proc. Natl. Acad. Sci. 114 (2017) E2293–E2302, https://doi.org/10.1073/PNAS.1612906114.
[35] T.E. Winkler, H. Ben-Yoav, S.E. Chocron, E. Kim, D.L. Kelly, G.F. Payne, R. Ghodssi, Electrochemical study of the catechol-modified chitosan system for clozapine treatment monitoring, Langmuir 30 (2014) 14686–14693, https://doi.org/10.1021/la503529k.
[36] R. Fernandes, X. Luo, C. Tsao, G.F. Payne, R. Ghodssi, G.W.R. De, W.E. Bentley, Biological nanofactories facilitate spatially selective capture and manipulation of quorum sensing bacteria in a bioMEMS device, Lab Chip 10 (2010) 1128–1134, https://doi.org/10.1039/b926846d.
[37] T. Gordonov, E. Kim, Y. Cheng, H. Ben-yoav, R. Ghodssi, G. Rubloff, J. Yin, G.F. Payne, W.E. Bentley, Electronic modulation of biochemical signal generation, Nat. Nanotechnol. 9 (2014) 605–610, https://doi.org/10.1038/nnano.2014.151.
[38] E. Kim, W.T. Leverage, Y. Liu, I.M. White, W.E. Bentley, G.F. Payne, Redox-capacitor to connect electrochemistry to redox-biology, Analyst 139 (2014) 32–43, https://doi.org/10.1039/c3an01632c.
[39] J. Li, D. Maniar, X. Qu, H. Liu, C. Tsao, E. Kim, W.E. Bentley, C. Liu, G.F. Payne, Coupling Self-Assembly Mechanisms to Fabricate Molecularly and Electrically Responsive Films, Biomacromolecules 20 (2019) 969–978, https://doi.org/10.1021/acs.biomac.8b01592.
[40] Y. Liu, C. Tsao, E. Kim, T. Tschirhart, J.L. Terrell, W.E. Bentley, G.F. Payne, Using a redox modality to connect synthetic biology to electronics : hydrogel-based chemo-electro signal transduction for molecular communication, Adv. Healthc. Mater. 6 (2017) 1600908, , https://doi.org/10.1002/adhm.201600908.
[41] W. Shang, Y. Liu, E. Kim, C. Tsao, G.F. Payne, W.E. Bentley, Selective assembly and functionalization of miniaturized redox capacitor inside microdevices for microbial toxin and mammalian cell, Lab Chip (2018) https://doi.org/10.1039/C8LC00583D.
[42] T. Tschirhart, X.Y. Zhou, H. Ueda, C.-Y. Tsao, E. Kim, G.F. Payne, W.E. Bentley, Electrochemical measurement of the β-Galactosidase reporter from live cells: a comparison to the miller assay, ACS Synth. Biol. 5 (2015) 28–35, https://doi.org/10.1021/acssynbio.5b00073.
[43] Y. Liu, E. Kim, I.M. White, W.E. Bentley, G.F. Payne, Information processing through a bio-based redox capacitor : signatures for redox-cycling, Bioelectrochemistry 98 (2014) 94–102, https://doi.org/10.1016/j.bioelechem.2014.03.012.
[44] Y. Cheng, X. Luo, J. Betz, S. Buckhout-White, O. Bekdash, G.F. Payne, W.E. Bentley, G.W. Rubloff, In situ quantitative visualization and characterization of chitosan electrodeposition with paired sidewall electrodes, Soft Matter 6 (2010) 3177, https://doi.org/10.1039/c0sm00124d.
[45] E. Kim, Y. Liu, X. Shi, X. Yang, W.E. Bentley, G.F. Payne, Biomimetic approach to confer redox activity to thin chitosan films, Adv. Funct. Mater. 20 (2010) 2683–2694, https://doi.org/10.1002/adfm.200902428.
[46] S.-Y. Cheng, S. Heilman, M. Wasserman, S. Archer, M.L. Shuler, M. Wu, A hydrogel-based microfluidic device for the studies of directed cell migration, Lab Chip 7 (2007) 763–769, https://doi.org/10.1039/b618463d.
[47] Y. Cheng, X. Luo, C. Tsao, H. Wu, J. Betz, G.F. Payne, W.E. Bentley, G.W. Rubloff, Biocompatible multi-address 3D cell assembly in microfluidic devices using spatially programmable gel formation, Lab Chip 11 (2011) 2316–2318, https://doi.org/10.1039/c1lc20306a.
[48] A.T. Lewandowski, H. Yi, X. Luo, G.F. Payne, R. Ghodssi, G.W. Rubloff, W.E. Bentley, Protein assembly onto patterned microfabricated devices through enzymatic activation of fusion pro-tag, Biotechnol. Bioeng. 99 (2008) 499–507, https://doi.org/10.1002/bit.
[49] X. Luo, A.T. Lewandowski, H. Yi, G.F. Payne, R. Ghodssi, W.E. Bentley, G.W. Rubloff, Programmable assembly of a metabolic pathway enzyme in a pre-packaged reusable bioMEMS device, Lab Chip 8 (2008) 420–430, https://doi.org/10.1039/b713756g.
[50] J.J. Park, X. Luo, H. Yi, R. Ghodssi, G.W. Rubloff, In situ biomolecule assembly and activity within completely packaged microfluidic devices, Lab Chip 6 (2006) 1315–1321, https://doi.org/10.1109/LSSA.2006.250370.
[51] L. Rover, J.C.B. Fernandes, G.D.O. Neto, L.T. Kubota, E. Katekawa, S.H.P. Serrano, Study of NADH stability using ultraviolet-visible spectrophotometric analysis and factorial design, Anal. Biochem. 260 (1998) 50–55, https://doi.org/10.1006/abio.1998.2656.
[52] K.M. Gray, B.D. Liba, Y. Wang, Y. Cheng, G.W. Rubloff, W.E. Bentley, A. Montembault, I. Royaud, L. David, G.F. Payne, Electrodeposition of a biopolymeric hydrogel: potential for one-step protein electroaddressing, Biomacromolecules 13 (2012) 1181–1189, https://doi.org/10.1021/bm3001155.
[53] E. Kim, T. Gordonov, Y. Liu, W.E. Bentley, G.F. Payne, Reverse engineering to suggest biologically relevant redox activities of phenolic materials, ACS Chem. Biol. 8 (2013) 716–724, https://doi.org/10.1021/cb300605s.
[54] R.T. Borchardt, I.J. Hidalgo, T.J. Raub, R.T. Borchardt, Characterization of the human Colon carcinoma cell line (Caco-2) as a model system for intestinal epithelial permeability, Gastroenterology 96 (2011) 736–749, https://doi.org/10.1208/s12248-011-9283-8 1989—The Backstory. AAPS J. 13, 323–327.
[55] V. Meunier, M. Bourrie, Y. Berger, G. Fabre, The human intestinal epithelial cell line Caco-2; pharmacological and pharmacokinetic applications, Cell Biol. Toxicol. 11 (1995) 187–194, https://doi.org/10.1007/BF00756522.
[56] G. Haslam, D. Wyatt, P.A. Kitos, Estimating the number of viable animal cells in multi-well cultures based on their lactate dehydrogenase activities, Cytotechnology 32 (2000) 63–75, https://doi.org/10.1023/A:1008121125755.
[57] A.J. Racher, D. Looby, J.B. Griffiths, Use of lactate dehydrogenase release to assess changes in culture viability, Cytotechnology 3 (1990) 301–307, https://doi.org/10.1007/BF00365494.
[58] H.T. Wolterbeek, A.J.G.M. van derMeer, Optimization, application, and interpretation of lactate dehydrogenase measurements in microwell determination of cell number and toxicity, Assay Drug Dev. Technol. 3 (2005) 675–682.
[59] S.T. Koev, P.H. Dykstra, X. Luo, G.W. Rubloff, W.E. Bentley, G.F. Payne, R. Ghodssi, Chitosan : an integrative biomaterial for lab-on-a-chip devices, Lab Chip 10 (2010) 3026–3042, https://doi.org/10.1039/c0lc00047g.
[60] B.D. Liba, E. Kim, A.N. Martin, Y. Liu, W.E. Bentley, G.F. Payne, Biofabricated film

with enzymatic and redox-capacitor functionalities to harvest and store electrons, Biofabrication 5 (2013) 015008,, , https://doi.org/10.1088/1758-5082/5/1/015008.

[61] E. Kim, Y. Liu, C.J. Baker, R. Owens, S. Xiao, W.E. Bentley, G.F. Payne, Redox-cycling and H2O2generation by fabricated catecholic films in the absence of enzymes, Biomacromolecules 12 (2011) 880–888, https://doi.org/10.1021/bm101499a.

[62] J.C.C. Haumeil, P.A. Rnaud, Evaluation of the cytotoxicity effect of dimethyl sulfoxide (DMSO) on Caco2 / TC7 Colon tumor cell cultures, Biol. Pharm. Bull. 25 (2002) 1600–1603, https://doi.org/10.1248/bpb.25.1600.

[63] C. Cao, E. Kim, Y. Liu, M. Kang, J. Li, J.-J. Yin, H. Liu, X. Qu, C. Liu, W.E. Bentley, G.F. Payne, Radical scavenging activities of biomimetic catechol-chitosan films, Biomacromolecules 19 (2018) 3502–3514, https://doi.org/10.1021/acs.biomac.8b00809.

[64] Y. Li, Y. Liu, E. Kim, Y. Song, C.-Y. Tsao, Z. Teng, T. Gao, L. Mei, W.E. Bentley, G.F. Payne, Q. Wang, Electrodeposition of a magnetic and redox-active chitosan film for capturing and sensing metabolic active bacteria, Carbohydr. Polym. 195 (2018) 505–514, https://doi.org/10.1016/J.CARBPOL.2018.04.096.

[65] Y. Wang, Y. Liu, E. Kim, B. Li, G.F. Payne, Electrochemical reverse engineering to probe for drug-phenol redox interactions, Electrochim. Acta 295 (2019) 742–750, https://doi.org/10.1016/J.ELECTACTA.2018.10.119.

[66] K. Yan, Y. Liu, Y. Guan, N. Bhokisham, C.-Y. Tsao, E. Kim, X.-W. Shi, Q. Wang, W.E. Bentley, G.F. Payne, Catechol-chitosan redox capacitor for added amplification in electrochemical immunoanalysis, Colloids Surf. B Biointerfaces 169 (2018) 470–477, https://doi.org/10.1016/J.COLSURFB.2018.05.048.